CORS Baade-Wesselink method in the Walraven photometric system: the period-radius and the period-luminosity relation of classical Cepheids

Molinaro, R.; Ripepi, V.; Marconi, M.; Bono, G.; Lub, J.; Pedicelli, S.; Pel, J. W.

Published in:
Monthly Notices of the Royal Astronomical Society

DOI:
10.1111/j.1365-2966.2010.18183.x

Publication date:
2011

Monthly Notices
of the
ROYAL ASTRONOMICAL SOCIETY

Mon. Not. R. Astron. Soc. **413,** 942–956 (2011) doi:10.1111/j.1365-2966.2010.18183.x

CORS Baade–Wesselink method in the Walraven photometric system: the period–radius and the period–luminosity relation of classical Cepheids

R. Molinaro,[1⋆] V. Ripepi,[1] M. Marconi,[1] G. Bono,[2,3,4] J. Lub,[5] S. Pedicelli[2] and J. W. Pel[6]

[1]*INAF–Osservatorio Astronomico di Capodimonte, Via Moiariello 16, 80131 Napoli, Italy*
[2]*Dipartimento di Fisica– Univ. di Roma Tor Vergata, via della Ricerca Scientifica 1, 00133 Roma, Italy*
[3]*INAF–Osservatorio Astronomico di Roma, Via Frascati 33, 00040 Monte Porzio Catone, Italy*
[4]*European Southern Observatory (ESO), Karl-Schwarzschild-Str. 2, D-85748 Garching bei München, Germany*
[5]*Leiden Observatory, Leiden University, PO Box 9513, 2300 RA Leiden, the Netherlands*
[6]*Kapteyn Institute, University of Groningen, PO Box 800, 9700 AV Groningen, the Netherlands*

Accepted 2010 December 10. Received 2010 December 9; in original form 2010 October 12

ABSTRACT

We present a new derivation of the CORS Baade–Wesselink method in the Walraven photometric system. We solved the complete Baade–Wesselink equation by calibrating the surface brightness function with a recent grid of atmosphere models. The new approach was adopted to estimate the mean radii of a sample of Galactic Cepheids for which are available precise light curves in the Walraven bands. Current radii agree, within the errors, quite well with Cepheid radii based on recent optical and near-infrared interferometric measurements. We also tested the impact of the projection factor on the period–radius relation using two different values ($p = 1.36$, 1.27) that bracket the estimates available in the literature. We found that the agreement of our period–radius relation with similar empirical and theoretical period–radius relations in the recent literature improves by changing the projection factor from $p = 1.36$ to 1.27. Our period–radius relation is $\log R = (0.75 \pm 0.03)\log P + (1.10 \pm 0.03)$, with an rms = 0.03 dex. Thanks to accurate estimates of the effective temperature of the selected Cepheids, we also derived the period–luminosity relation in the V band and we found $M_V = (-2.78 \pm 0.11)\log P + (-1.42 \pm 0.11)$ with rms = 0.13 mag, for $p = 1.27$. It agrees quite well with recent results in the literature, while the relation for $p = 1.36$ deviates by more than 2σ. We conclude that, even taking into account the intrinsic dispersion of the obtained period–luminosity relations that is roughly of the same order of magnitude as the effect of the projection factor, the results of this paper seem to favour the value $p = 1.27$.

Key words: stars: variables: Cepheids.

1 INTRODUCTION

Classical Cepheids are fundamental standard candles to determine both Galactic and extragalactic distances. They obey well-defined optical and near-infrared period–luminosity and period–luminosity–colour relations. Thanks to the unprecedented spatial resolution of the *Hubble Space Telescope* (*HST*), Cepheids can be used as primary distance indicators up to the Virgo cluster (≈25 Mpc). This means that they can also be adopted to provide robust absolute calibrations of secondary distance indicators, and in turn to estimate the value of the Hubble constant (see e.g. Freedman et al. 2001).

The accuracy reached in the determination of cosmological parameters using the Cepheid distance scale relies on the knowledge of the physical mechanisms that govern their radial oscillations and on their dependence on intrinsic parameters [luminosity, mass, radius, chemical composition; see e.g. Bono, Marconi & Stellingwerf (1999, 2000); Bono, Castellani & Marconi (2002); Keller & Wood (2006), and references therein]. In particular, the estimate of Cepheid radii and of the effective temperature (using mean intrinsic colours) allows us to constrain their intrinsic luminosity. Furthermore, the Cepheid mass can be estimated by adopting a period–mass–radius relation (see e.g. Bono et al. 2001b, and references therein), and in turn to provide independent constraints on the mass–luminosity relations.

The methods currently used to derive Cepheid radii from photometric and spectroscopic data (radial velocity) are based on the classical Baade–Wesselink technique (Wesselink 1946). Among them,

⋆E-mail: molinaro@na.astro.it

the surface brightness technique (Barnes & Evans 1976) and the CORS method (Caccin et al. 1981) rely on solid physical bases. The reader interested in a detailed discussion concerning the different Baade–Wesselink methods is referred to Gautschy (1987). The use of interferometric methods and the measurement of parallaxes provide a model-independent method for radius measurements. However, this approach has only been applied to a very limited sample of bright nearby Cepheids (Nordgren et al. 2000; Lane, Creech-Eakman & Nordgren 2002; Kervella et al. 2004; Davis et al. 2009). On the other hand, the Baade–Wesselink methods can be applied to large samples of Cepheids, and it has been recently extended to Magellanic Cepheids (Storm et al. 2005). However, the precision of Baade–Wesselink distances strongly depends on the quality of photometric and radial velocity data.

In a previous paper (Ruoppo et al. 2004), we adapted the CORS method to derive Cepheid radii observed in the Strömgren system. However, the model atmospheres adopted in the quoted investigation to estimate the surface brightness did not allow us to include Cepheids with periods longer than 12–13 d. The cut-off in the long-period range limited the accuracy of the period–radius relation.

Recently, Pedicelli et al. (2009) provided new calibrations based on a new release of model atmospheres by Castelli (1999) for the Walraven photometry of Galactic Cepheids originally collected by Pel (1978). The Walraven system includes five bands (V, B, L, U, W) designed to measure the features of hydrogen spectrum. Three of them have the central wavelength in the ultraviolet region (see Lub & Pel 1977; Pel & Lub 2007, for more details about this photometric system). In particular, the central wavelengths of the Walraven filters are the following: $\lambda_V = 5405, \lambda_B = 4280, \lambda_L = 3825, \lambda_U = 3630, \lambda_W = 3240$ Å.

In this investigation, we show that this new calibration of the *VBLUW* Cepheid time series data by Pedicelli et al. (2009) allows us to derive precise stellar parameters (surface gravity and effective temperature) at fixed chemical composition and to calibrate with high accuracy the surface brightness function, a fundamental ingredient for the application of the Baade–Wesselink method. This opportunity stimulated us to apply the CORS version of the Baade–Wesselink technique as formulated by Onnembo et al. (1985) and Ruoppo et al. (2004), to derive reliable radii for a sample of Cepheids having periods from a few days up to ∼40 d and to obtain more accurate period–radius and period–luminosity relations.

The layout of the paper is as follows. The original CORS method is introduced in Section 2. The grids of atmosphere models and the calibration of the surface brightness in the Walraven system are described in Section 3. In Section 4 we describe the adopted photometric and spectroscopic data, while the estimate of the Cepheids radii and of the period–radius relation are discussed in Sections 5 and 6, respectively. In Section 7 we discuss the derivation of the period–luminosity relation. Finally, Section 8 summarizes the main results of this investigation.

2 THE CORS METHOD

The original CORS method (Caccin et al. 1981) is a variant of the classical Baade–Wesselink technique (Wesselink 1946) and was developed to derive the radii of pulsating stars. It relies on the surface brightness function:

$$S_V = m_V + 5 \log \alpha, \tag{1}$$

where m_V is the apparent visual magnitude and α is the angular diameter of the star. For a variable star, equation (1) can be written for each phase (ϕ) along the pulsational cycle. By differentiating the above equation with respect to the phase, by multiplying the result with a colour index (C_{ij}, where ij are two generic photometric bands) and by integrating over the entire cycle, one can write

$$q \int_0^1 \ln \left\{ R_0 - pP \int_{\phi_0}^{\phi} v(\phi')\, \mathrm{d}\phi' \right\} C'_{ij}\, \mathrm{d}\phi - B + \Delta B = 0, \tag{2}$$

where $q = 5/\ln 10$, P is the period, v is the radial velocity and p is the radial velocity projection factor. The other two terms, B and ΔB, are the following:

$$B = \int_0^1 C_{ij}(\phi) m'_V(\phi)\, \mathrm{d}\phi \tag{3}$$

$$\Delta B = \int_0^1 C_{ij}(\phi) S'_V(\phi)\, \mathrm{d}\phi\ . \tag{4}$$

The projection factor p correlates radial and pulsation velocity, i.e. $R'(\phi) = -pPv(\phi)$. The uncertainty affecting the estimates of this parameter is still the main source of systematic errors in the Baade–Wesselink method. We shall discuss the p value in Section 5.1.

By solving equation (2) we estimate the value of the radius R_0 at an arbitrary phase ϕ_0, while the radius at any phase ϕ along the pulsational cycle can be evaluated by integrating the radial velocity curve between ϕ_0 and ϕ. The term B present in equation (2) can be easily determined using colour and magnitude (B), while the term ΔB is not directly connected to observational data, but approximates the area of the loop performed by variable stars in the colour–colour plane.

Typically the ΔB term has a small value (10^{-3}–10^{-4}; Onnembo et al. 1985) and in the original Baade–Wesselink method it is neglected (see Caccin et al. 1981). However, the Cepheid radii estimated by including the ΔB term in the equation (2) are more accurate than those based on the original Baade–Wesselink method (Sollazzo et al. 1981; Ripepi et al. 1997, 2000; Ruoppo et al. 2004).

In the next section we describe how to calibrate the surface brightness function to estimate the term ΔB from equation (4).

3 THE MODIFIED CORS METHOD

3.1 The grids of atmosphere models

In order to calibrate the surface brightness function, we assume the validity of the quasi-static approximation (QSA)[1] for the Cepheid atmosphere (see also Onnembo et al. 1985). Under this hypothesis, any photometric quantity can be expressed as a function of effective temperature and gravity ($T_{\rm eff}$, $g_{\rm eff}$). Then, we can write

$$S_V = S_V(T_{\rm eff},\ g_{\rm eff}) \tag{5}$$

for the surface brightness, and

$$\begin{aligned} C_{ij} &= C_{ij}(T_{\rm eff},\ g_{\rm eff}) \\ C_{kl} &= C_{kl}(T_{\rm eff},\ g_{\rm eff}) \end{aligned} \tag{6}$$

for two intrinsic colour indices. If the determinant of the Jacobian $J(C_{ij}, C_{kl}|T_{\rm eff}, g_{\rm eff}) \neq 0$, the last two equations can be inverted and we obtain:

$$\begin{aligned} T_{\rm eff} &= T_{\rm eff}(C_{ij},\ C_{kl}) \\ g_{\rm eff} &= g_{\rm eff}(C_{ij},\ C_{kl}) \end{aligned} \tag{7}$$

[1] The QSA assumes that the atmosphere of the pulsating star can be described, at any time, by a classical hydrostatic, plane-parallel model in radiative/convective equilibrium and in local thermodynamic equilibrium, identified by the effective temperature ($T_{\rm eff}$) and by the effective gravity ($g_{\rm eff} = \frac{GM}{R^2} + \frac{\mathrm{d}^2 R}{\mathrm{d}t^2}$).

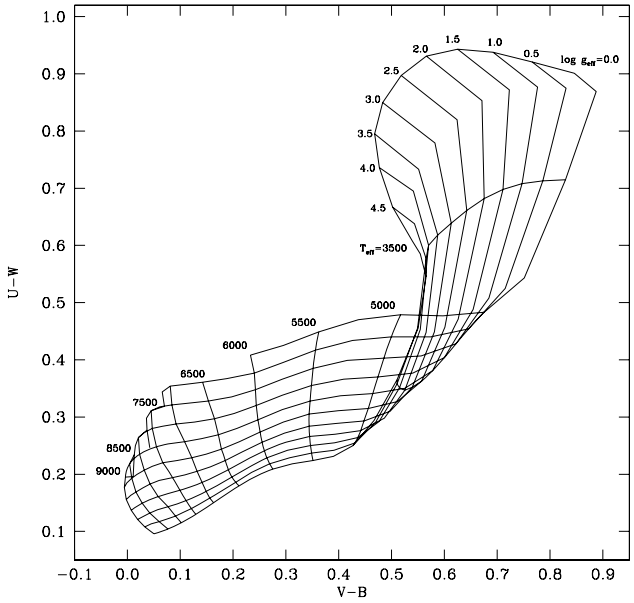

Figure 1. The grids of model atmosphere plotted in the plane of $(V - B)$, $(U - W)$ colours: lines of constant temperature and constant gravity are plotted.

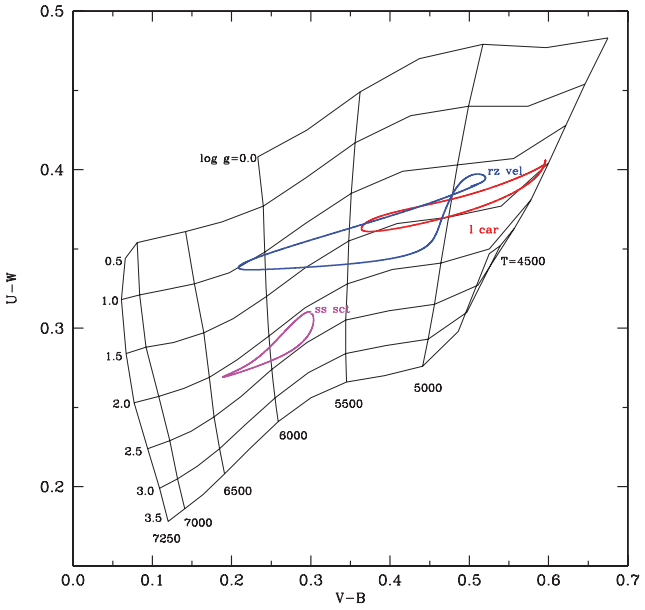

Figure 2. Colour–colour loops for three selected Cepheids plotted on to the theoretical grids. The three Cepheids are SS Sct ($P = 3.7$ d), RZ Vel ($P = 20.4$ d) and l Car ($P = 35.5$ d).

and, we can also write the surface brightness as a function of the two colour indices:

$$S_V = S_V(C_{ij},\ C_{kl}). \tag{8}$$

In general, the invertibility condition is not valid over the entire parameter space, since the same pair of colours trace different pairs of gravity and temperature ($g_{\rm eff}, T_{\rm eff}$). Fig. 1 shows the colour degeneracy present in the grid of atmosphere model provided by Castelli (1999) (http://wwwuser.oat.ts.astro.it/castelli/colors/vbluw.html), for the Walraven two-colour diagram $(V - B)$ versus $(U - W)$[2].

However, a local solution can be found, provided that an appropriate choice of the colours C_{ij} and C_{kl} and of the range in colour is made. By using the quoted colours $(V - B)$ and $(U - W)$, we succeeded in inverting equation (6) for the range of parameters typical of Cepheids, i.e. $0.0 \leq \log g_{\rm eff} \leq 3.0$ dex and $4500 \leq T_{\rm eff} \leq 7250$ K.

To verify that real Cepheids are located inside the theoretical grid, we plotted the loops, obtained by fitting the observed colours of selected Cepheids, in the quoted colour–colour plane. The result for three Cepheids with short-, medium- and long-period, is shown in Fig. 2. A glance at the data plotted in this figure shows that the three loops performed by actual Cepheids are located inside the limits of the predicted grid.

Lub & Pel (1977) and Pel (1978) pointed out that the flux in the W band was measured with sufficient accuracy only for the brightest Cepheids due to the intrinsic faintness of Cepheid fluxes in the near-ultraviolet, but also because the telescope mirror reflectivity in this band was deteriorated at the epoch of observations. Therefore, we decided to perform a further test by using the pair of colours $(V - B)$ and $(L - U)$, even if the curves of constant temperature and gravity are not orthogonal as in the plane with the $(U - W)$ colour. Accurate solutions can be obtained in the range $5000 \leq T_{\rm eff} < 7500$ K and $0.0 \leq \log g_{\rm eff} \leq 4.00$ dex. However, the loops of Cepheids with periods longer than 11 d fall outside the grid of models. This means that the structural parameters of Cepheids and the surface brightness function are less accurate using this colour–colour plane. Nevertheless, the ratios of the Cepheid radii with $P < 11$ d, estimated using the two different colour–colour planes, show that the differences are smaller than 10 per cent. On the basis of this evidence, we decided to focus our attention on the $(V - B)$–$(U - W)$ plane (see Appendix B for more details).

[2] We remember that in the Walraven photometric system the magnitude in a generic band X is defined without the -2.5 factor: $m_X = \log F_X$. As a consequence, the colour is defined as the difference between the magnitude at longer and at shorter wavelength.

3.2 Derivation of S_V

The availability of a region across the theoretical grid covering the locus occupied by the Cepheid colour–colour loops and the validity of the invertibility condition shown in the above section provide us with an instrument to write effective temperature and gravity as a function of the two colour indices and, finally to calibrate the surface brightness through equation (8).

As a first step, we have fitted the theoretical grid shown in Fig. 2 by means of polynomials, in order to express temperature and gravity as a function of $(V - B)$ and $(U - W)$ colours, according to equation (7) (see Appendix A for details about the fitted equations). The surfaces $\log T_{\rm eff} = \log T_{\rm eff}(V - B, U - W)$ and $\log g_{\rm eff} = \log g_{\rm eff}(V - B, U - W)$ are shown in Figs 3 and 4. The rms around the fitted equations amount to 0.0033 and 0.15 dex for $\log T_{\rm eff}$ and $\log g_{\rm eff}$, respectively.

Following the Walraven convention for magnitudes, the surface brightness can be derived in the following way:

$$S_V = \text{const.} + 4 \log T_{\rm eff} - \text{BC}(T_{\rm eff},\ g_{\rm eff}), \tag{9}$$

where BC is the bolometric correction calculated as a function of $T_{\rm eff}$ and $g_{\rm eff}$ through a polynomial fit (see Appendix A). A plot of the fit of BC as a function of $\log T_{\rm eff}$ and $\log g_{\rm eff}$ is shown in Fig. 5.

The procedure described here allows us to calculate the term ΔB in the complete CORS formulation (equation 2).

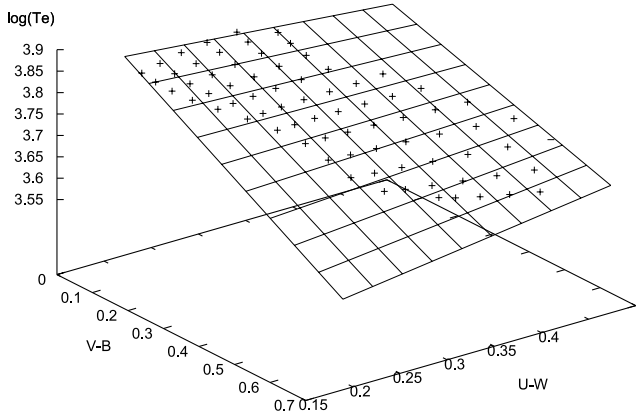

Figure 3. The surface representing $\log T_{\rm eff}$ as a function of $(V - B)$ and $(U - W)$, obtained from the polynomial fit of the atmosphere models (crosses) from Castelli (1999).

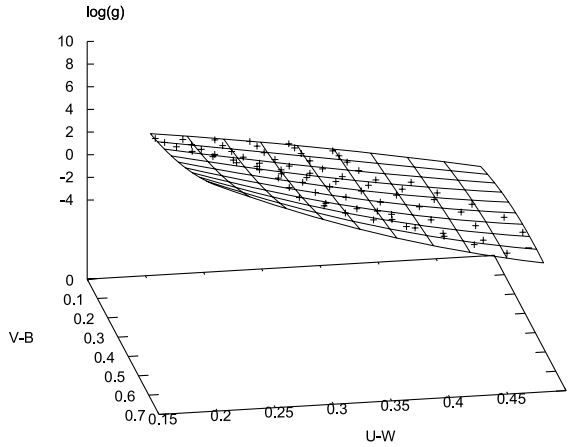

Figure 4. The same as Fig. 3, but for $\log g_{\rm eff}$.

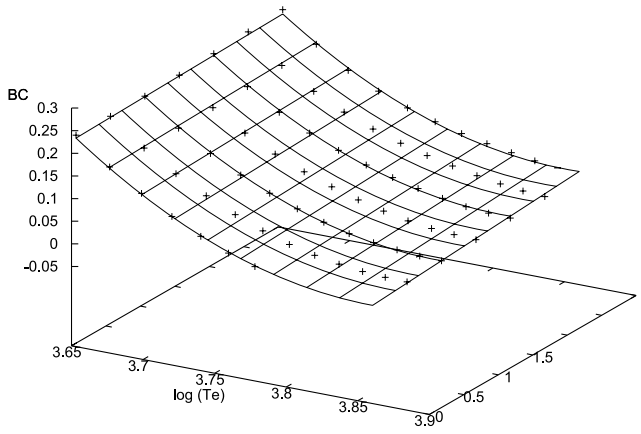

Figure 5. The surface representing the Bolometric Correction, BC, as a function of $\log T_{\rm eff}$ and $\log g_{\rm eff}$, obtained from the polynomial fit of atmosphere models (crosses) from Castelli (1999).

3.3 Test with spectroscopic and interferometric data

In the previous section, we have described the procedure followed to derive the physical parameters of Cepheids starting from the measured colours. In order to test the accuracy of the fitted relations (equation 7), we have performed a comparison of the effective temperature and gravity derived from the fitted relations for selected Cepheids in our sample with the results obtained by other authors using an independent spectroscopic approach.

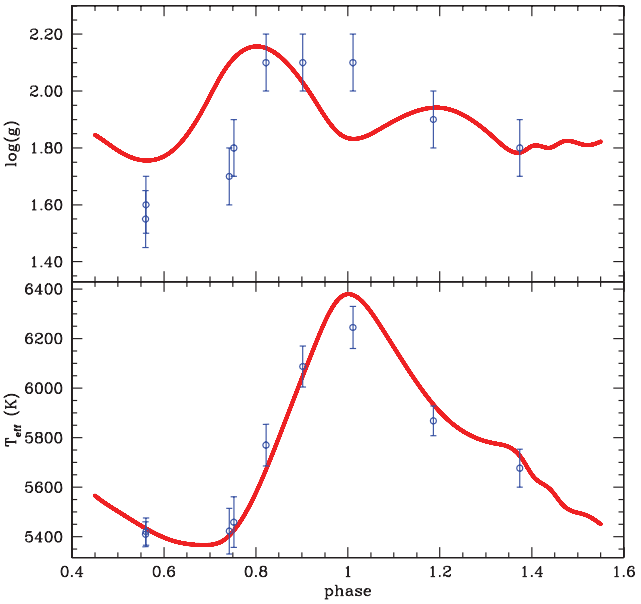

Figure 6. Effective temperature (bottom panel) and gravity (upper panel), obtained by fitting the grid of model atmosphere, are plotted as function of the pulsational phase for the star U Sgr ($P = 7.9$ d). The open blue circles with the associated error bars represent the values of the physical parameters obtained spectroscopically by Luck & Andrievsky (2004).

As an example, in Fig. 6 we have plotted the values of effective temperature and gravity obtained with our equations for the pulsational cycle of the Cepheid U Sgr. In the same figure we also overplotted the values of the physical parameters obtained spectroscopically by Luck & Andrievsky (2004) using the line depth ratios. We note that the curve of effective temperature follows the spectroscopic data with great accuracy. The agreement is less satisfactory for the curve of gravity, probably as a consequence of the cited problems with the W band. Similar results are obtained for another dozen of stars for which the comparison with spectroscopic data was possible. We can conclude that our approximation for the effective temperature is quite accurate, with mean relative differences of 0.4 per cent. On the other hand, we can reproduce the effective gravity, $\log g_{\rm eff}$, with mean relative differences of 4 per cent. However, the larger error affecting the estimate of the surface gravity is not a thorny problem in the estimate of Cepheid radii, because the gravity enters only in the determination of the ΔB term, through the contribution of the BC to the surface brightness (S_V). The ΔB term contributes at most with a 5 per cent to the radius, therefore we can conclude that even a significant uncertainty in our determination of the gravity has a minimal impact on the determination of Cepheid radii.

As a further test of the accuracy of our approximation for the surface brightness S_V, we have compared the angular diameter θ of l Car (which is the only single Cepheid for which this comparison is possible) obtained through interferometric measurements (Kervella et al. 2004; Davis et al. 2009) with those obtained from the surface brightness equation:

$$\theta(\phi) = 10^{0.2[S_V(\phi) - m_V(\phi)]}, \qquad (10)$$

where ϕ is the phase along the pulsational cycle and θ is given in mas (see Fig. 7). A glance at the figure shows that current solution

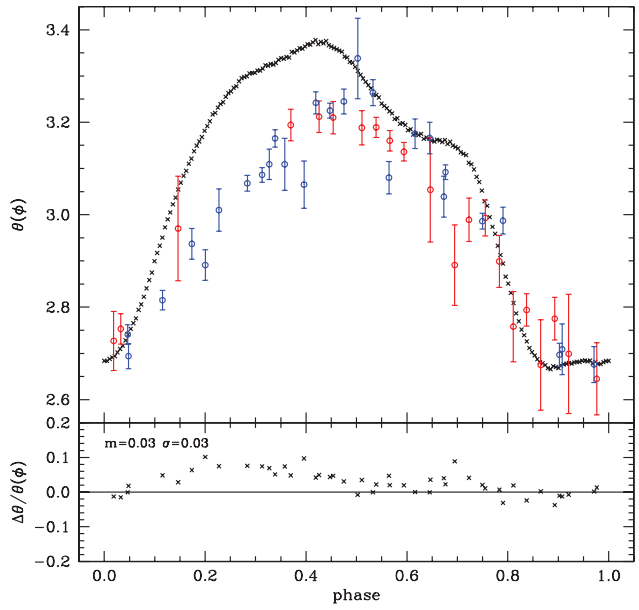

Figure 7. Top panel: the curve of angular diameter θ (in mas) of l Car, obtained from the surface brightness calibration using equation 10 (black points), is plotted with the interferometric measurements obtained by Kervella et al. (2004) (red points) and by Davis et al. (2009) (blue points). Bottom panel: difference between the two curves the mean and standard deviation of such a difference is labelled.

shows a systematic difference with the interferometric measurements in the phase range between 0.2 and 0.45. This discrepancy is due to the limited accuracy of the calibration we are using to estimate the surface gravity. Typically, current calibration underestimates the gravity, in the above phase interval, and in turn overestimates the radius. The reader interested in a thorough analysis of this problem is referred to Pel (1978). He suggested that the main culprit of the above discrepancy is the fact that we use grid of atmosphere models that neglect the microturbulence variation along the pulsation cycle. Furthermore, the problem in the W-band reflectivity, described above, also affects the surface gravity calibration. However, it is worth mentioning that a detailed analysis of the residuals between current estimates and interferometric measurements indicate a mean difference and a dispersion of the order of 3 per cent.

Assuming that the interferometric measurements are minimally affected by systematic errors, we can use this average difference to estimate our systematic indetermination on S_V through equation 1, obtaining a value of $\sim$8 per cent. Recalling that S_V enters only in the determination of the ΔB, which in turn is only $\sim$5 per cent of the radius, we found that the systematic uncertainty on our estimate of S_V implies a 0.4 per cent uncertainty on the radius.

The agreement between the physical parameters obtained with our procedure and those obtained independently from spectroscopy and interferometry seems a valuable test of the accuracy in the derivation of the surface brightness and of the ΔB term, thus supporting the soundness of our approach.

4 PHOTOMETRIC AND SPECTROSCOPIC DATA

After the validation of the quoted approach, we applied it to real data in order to obtain the radii of a sample of classical Galactic Cepheids.

The photometric data and the radial velocities used in this work are described in the following.

4.1 Photometric data

The original sample we have used in this work includes 175 Cepheids observed in the Walraven *VBLUW* photometric system during 1962 and 1970–71 at the Leiden Southern Station (South Africa) (Walraven, Tinbergen & Walraven 1964; Pel 1976). It is 82 per cent complete for all Cepheids brighter than $V = 11.0$ mag at minimum of the light curve and with declination lower than $+15^\circ$.

We have selected all the type I Cepheids (163 stars) included in this sample, but we have retained only those stars for which reliable radial velocity data were available in the literature (see next section). Furthermore, we have rejected also those stars having the colour–colour loop at least in part outside the grid of models. This behaviour can be observed for Cepheids having an extremely large loop or a loop with a peculiar orientation in the colour–colour plane (abnormal loop orientations can be caused by the presence of companions or by peculiar chemical abundances). A complete list of the selected stars, with the photometric parameters used in this work, is shown in Table 1.

Before using the photometric data, we have corrected the colours for the reddening effect following the procedure described in Pedicelli et al. (2008). In particular, we have obtained the colour excess $E(V - B)$ in the Walraven system from:

$$\frac{E(B-V)_J}{E(V-B)} = 2.375 - 0.169(V-B), \qquad (11)$$

where $(V - B)$ is the mean[3] Walraven colour of the considered star and $E(B - V)_J$ is the colour excess in the Johnson system. As for the colour excess in the Johnson filters, we have referred to Laney & Caldwell (2007) or to Fernie et al. (1995) when the value was not available in the former work. In the latter case, we have transformed the value of the colour excess from the Fernie's scale into the Laney & Caldwell scale by using the relation recently provided by Fouqué et al. (2007), namely $E(B - V)_{\rm L\&C} = 0.952E(B - V)_{\rm Fernie}$ mag. The $(U - W)$ colour excesses follow from the relation $E(U - W) = 0.45E(V - B)$ (Pedicelli et al. 2008).

4.2 Radial velocity data

We have obtained the radial velocity data from different sources available in the literature. The references of radial velocity data are listed in Table 1 for each star of the sample.

The main catalogues used in this work are from Stibbs (1955), Gieren (1977, 1981, 1985), Coulson et al. (1985), Barnes et al. (1987, 1988), Metzger et al. (1993), Bersier et al. (1994), Taylor et al. (1997), Gorynya et al. (1998), Imbert (1999), Bersier (2002) and Storm et al. (2004). The sample of radial velocity measurements was selected according to the following criteria. We neglected Cepheids with less than 10 measurements. For the Cepheids with multiple samples of radial velocity measurements, we selected the data set characterized either by the most accurate measurements – typically better than $\sim$1 km s^{-1} – and/or closer in time with photometric data. The latter criterion was adopted to minimize possible problems due to period changes and/or phase of maxima that are not very precise. In a few cases (nine stars), we have combined two

[3] The mean is derived by applying the integral mean value theorem to the colour curve.

Table 1. The names of Cepheids used in this work together with their period are listed in the first and second columns, respectively. The third and fourth columns contain respectively the colour excess $E(B-V)$ in the Johnson system, from Laney & Caldwell (2007) (L) or those from Fernie et al. (1995) (F) transformed in the Laney and Caldwell system by using the relation from Fouqué et al. (2007) and the $E(V-B)$ in the Walraven system calculated from equation (11). In the last column, we list the source of the radial velocity data and, when more than one source is taken into account the shift in radial velocity (km s^{-1}), if any, is given in parentheses.

Star	Period (d)	$E(B-V)$ (Johnson)	$E(V-B)$ (Walraven)	Radial velocity
η Aql	7.1766	0.126 (L)	0.064	Barnes, Moffet & Slovak (1987)
FM Aql	6.1142	0.583 (L)	0.283	Gorynya et al. (1998)
FN Aql	9.4822	0.491 (L)	0.214	Gorynya et al. (1998)
TT Aql	13.7546	0.417 (L)	0.217	Bersier (2002)
U Aql	7.0239	0.351 (L)	0.173	Bersier (2002)
V496 Aql	6.8070	0.383 (L)	0.167	Gieren (1981)
RY CMa	4.6782	0.254 (L)	0.110	Barnes, Moffet & Slovak (1988)(+0.5), Gorynya et al. (1998)
SS CMa	12.3620	0.590 (L)	0.258	Coulson, Caldwell & Gieren (1985)
AQ Car	9.7690	0.173 (L)	0.07	Coulson et al. (1985)
ER Car	7.7187	0.096 (F)	0.042	Lloyd Evans (1980)(+0.4), Stibbs (1955)
l Car	35.5330	0.138 (L)	0.075	Taylor et al. (1997)
U Car	38.7681	0.260 (L)	0.124	Coulson et al. (1985)
V Car	6.6967	0.170 (L)	0.075	Stibbs (1955)
VY Car	18.9213	0.218 (L)	0.106	Coulson et al. (1985)
XX Car	15.7162	0.361 (L)	0.157	Coulson et al. (1985)
XY Car	12.4348	0.416 (L)	0.182	Coulson et al. (1985)
AZ Cen	3.2107	0.159 (L)	0.068	Gieren (1981)
V Cen	5.4939	0.305 (L)	0.125	Bersier (2002)
V339 Cen	9.4672	0.415 (L)	0.181	Coulson et al. (1985)
XX Cen	10.9558	0.267 (L)	0.116	Coulson et al. (1985)
AG Cru	3.8373	0.171 (L)	0.074	Gieren (1981)(+4.2), Stibbs (1955)
S Cru	4.6900	0.144 (L)	0.062	Gieren (1981)
X Cru	6.2200	0.272 (F)	0.118	Bersier (2002)
W Gem	7.9141	0.253 (L)	0.123	Imbert (1999)
SV Mon	15.2321	0.220 (L)	0.108	Imbert (1999)
R Mus	7.5099	0.114 (F)	0.049	Lloyd Evans (1980)
UU Mus	11.6364	0.414 (L)	0.180	Bersier (2002)
S Nor	9.7549	0.180 (L)	0.078	Bersier et al. (1994)
U Nor	12.6413	0.816 (L)	0.396	Coulson et al. (1985)
BF Oph	4.0678	0.223 (L)	0.096	Gieren (1981)
Y Oph	17.1241	0.660 (L)	0.290	Gorynya et al. (1998)
RS Ori	7.5668	0.363 (L)	0.169	Gorynya et al. (1998), Imbert (1999)(−0.3)
AP Pup	5.0843	0.198 (F)	0.086	Stibbs (1955)
AT Pup	6.6650	0.207 (L)	0.089	Gieren (1985)
RS Pup	41.3876	0.454 (L)	0.197	Storm et al. (2004)
X Pup	25.9610	0.404 (L)	0.177	Barnes et al. (1988)
WX Pup	8.9382	0.303 (L)	0.138	Stibbs (1955), Barnes et al. (1988)(−1.7)
RV Sco	6.0613	0.365 (L)	0.158	Lloyd Evans (1980)(+2.9), Gieren (1981), Stibbs (1955)(−1.1)
V482 Sco	4.5279	0.334 (L)	0.145	Gieren (1981)
V500 Sco	9.3166	0.618 (L)	0.263	Stibbs (1955)
V636 Sco	6.7966	0.207 (F)	0.089	Stibbs (1955)
EV Sct	3.0910	0.703 (L)	0.300	Metzger et al. (1993)(+0.4), Bersier et al. (1994)(+0.4), Storm et al. (2004)
SS Sct	3.6712	0.324 (L)	0.140	Gieren (1981)
X Sct	4.1981	0.589 (F)	0.257	Metzger et al. (1993)
Y Sct	10.3415	0.751 (L)	0.364	Barnes et al. (1988)
AP Sgr	5.0579	0.179 (L)	0.077	Gieren (1981)
BB Sgr	6.6370	0.302 (L)	0.131	Gieren (1981)
U Sgr	6.7449	0.408 (L)	0.176	Bersier et al. (1994)
X Sgr	7.0122	0.284 (L)	0.122	Wilson et al. (1989)
Y Sgr	5.7733	0.187 (L)	0.089	Bersier (2002)
YZ Sgr	9.5534	0.286 (L)	0.127	Lloyd Evans (1980); Barnes et al. (1988)
W Sgr	7.5947	0.103 (L)	0.048	Bersier et al. (1994)
R TrA	3.3893	0.144 (L)	0.054	Gieren (1981)
S TrA	6.3234	0.081 (L)	0.035	Lloyd Evans (1980)(+1.4), Gieren (1981)
AH Vel	4.2271	0.070 (F)	0.030	Gieren (1977)
AX Vel	2.5929	0.239 (L)	0.103	Stibbs (1955)
BG Vel	6.9236	0.426 (F)	0.186	Stibbs (1955)
RY Vel	28.1270	0.545 (L)	0.240	Coulson et al. (1985)

Table 1 – *continued*

Star	Period (d)	$E(B-V)$ (Johnson)	$E(V-B)$ (Walraven)	Radial velocity
RZ Vel	20.3969	0.294 (L)	0.129	Coulson et al. (1985)
SX Vel	9.5499	0.274 (L)	0.108	Stibbs (1955)
SW Vel	23.4744	0.346 (L)	0.153	Coulson et al. (1985)
T Vel	4.6397	0.289 (L)	0.122	Stibbs (1955)
V Vel	4.3710	0.144 (L)	0.090	Gieren (1985)

or more data sets in order to improve the sampling along the radial velocity curve. To accomplish this goal, we corrected for possible shifts in radial velocity among the different data sets. The shift was determined by interpolating the most accurate sample of radial velocities and then by estimating the median distance – along the velocity axis – between the fitted curve and the other radial velocity samples. The values of the shift we found are listed in Table 1.

In order to obtain an accurate phasing between the photometric and spectroscopic data, we recalculated the phases of radial velocity measurements by using the same epoch and period as for the photometry. The final sample used in this work consists of 63 Cepheids whose main characteristics are listed in Table 1.

5 DERIVATION OF THE RADIUS OF CEPHEIDS

5.1 The projection factor *p*

Using the photometric data and the radial velocities discussed in the previous section, we are able to derive the mean radius for each star of our sample following the procedure introduced in Sections 2 and 3. However, before proceeding we have to fix the value of the projection parameter p. In the recent literature, there is a strong debate about the correct value to use for this important parameter. Moreover, it is not clear yet if p is constant over the entire period range covered by the Cepheids. A detailed review of this subject can be found in Barnes (2009) and there is no need to repeat here the discussion outlined in that paper, but the conclusion that can be drawn is that the p value is uncertain at a level of 5–10 per cent. The same uncertainties apply to the possible dependence of p on the Cepheid pulsation period. As a matter of fact, several authors find either a mild (see e.g. Nardetto et al. 2007, 2009) or a strong (see e.g. Barnes 2009) dependence on period. On the contrary, Groenewegen (2007), using Cepheids with *HST* parallaxes (Benedict et al. 2007) and interferometrically measured angular diameters, find, convincingly, a value of $p = 1.27 \pm 0.05$ with no dependence on the period. The same result ($p = 1.27 \pm 0.06$) was found geometrically for δ Cephei by using interferometric measurements, obtained with the CHARA Array, and published parallax (Mérand et al. 2005).

Moreover, the projection factor p is usually assumed to be constant along the pulsation cycle. However, this assumption was questioned by Ripepi et al. (1997), since by using the changes of p predicted by Sasselov & Karovska (1994), they found that the radius determinations change by approximately 6 per cent. The change of the p factor along the cycle has been the crossroad of several theoretical (Marengo et al. 2002) and empirical (Nardetto et al. 2004) investigations, but we still lack firm quantitative estimates of the changes. This is the reason why it is neglected in recent estimates of the Cepheid radii. We also neglected this change to perform comparison with similar data available in the literature.

Given this overall uncertainty, we decided to use two different values of the p factor: 1.36 and 1.27. These two values were chosen because they include the range of values found in the literature and, in particular, the value 1.36 was selected to allow comparison with our previous works (Ripepi et al. 1997; Ruoppo et al. 2004).

Table 2. Interferometric radii derived by Kervella et al. (2004) compared with the results of this work for $p = 1.36$. In the first column there is the name of the Cepheids in common with the sample of Kervella et al., while in the second and third columns there are the interferometric radius and our estimation, respectively.

Star	Kervella et al.	This work
X Sgr	52.2^{+23}_{-12}	$52.4^{+3.7}_{-3.5}$
η Aql	$59.3^{+5.3}_{-4.6}$	$59.0^{+4.5}_{-4.2}$
W Sgr	56.4^{+30}_{-16}	$53.4^{+4.1}_{-3.8}$
Y Oph	136^{+325}_{-56}	$90.7^{+6.9}_{-6.4}$
l Car	$191.2^{+7.6}_{-6.0}$	$190.7^{+13.6}_{-12.7}$

5.2 Radius calculation

The FORTRAN77 code used in this work performs a fit of the magnitude curve, the $(V-B)$, $(U-W)$ colour curves and the radial velocity curve using a Fourier fit, with a number of harmonics fixed interactively by the user. Then it solves the CORS equation (2) for the radius at an arbitrary phase both with and without the ΔB term. The mean radius is, finally, calculated by integrating the radial velocity curve twice.

Tables 2 and 3 gives the results of our procedure together with the radii obtained by other authors. For three stars, the CORS procedure does not converge and consequently the radius is not available. In particular, we have listed the name of the star, information on binarity, the period, the radius obtained with and without the ΔB term and some results found in the literature (Rojo Arellano & Arellano Ferro 1994; Ruoppo et al. 2004; Barnes et al. 2005). In order to perform the comparison with similar estimates available in the literature, we rescaled their radius determinations according to our value of the projection factor. We found that our radius determinations agree quite well with those provided by Rojo Arellano & Arellano Ferro (1994), with a median difference of less than 1 per cent and a dispersion of 15 per cent. On the other hand, current radius evaluations are $\sim$13 per cent smaller than those provided by Ruoppo et al. (2004) and $\sim$21 per cent larger than those by Barnes et al. (2005), with a dispersion of the order of 14 per cent for both of them.

As further test, we have selected the Cepheids of our sample with available interferometric measurements of the radius. In particular, we compared the radii contained in Kervella et al. (2004), obtained with $p = 1.36$, with our results corresponding to the same projection factor. The stars in common with their sample are X Sgr, η Aql, W

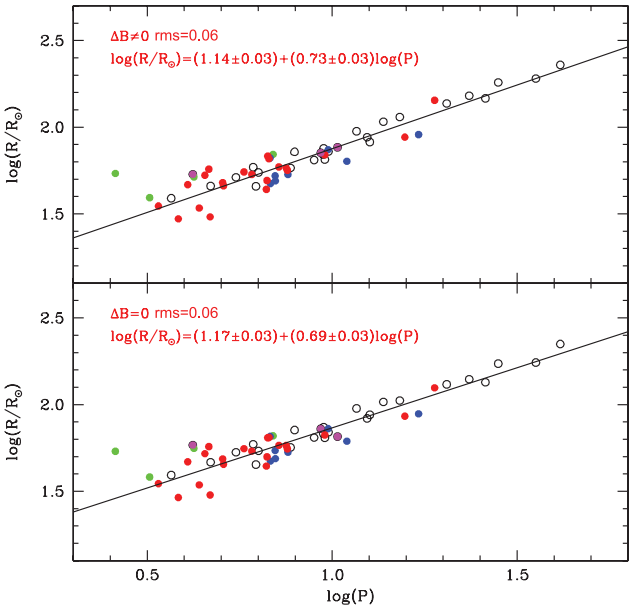

Figure 8. Period–radius relations obtained in the case with ΔB term (bottom panel) and without ΔB term (upper panel), using all the Cepheids of our sample, with the exception of first overtone pulsators (green points). Single stars and visual binaries are plotted as black circles, spectroscopic binaries as red points, spectroscopic binaries with known orbit as blue points and binaries with photometric companion with unknown physical relations as magenta points.

Sgr, Y Oph and l Car. As shown in Table 2, our radii are completely consistent with interferometric measurements, except for Y Oph, but the error given by Kervella et al. is extremely large.

We found another estimation of the radius of l Car and η Aql in Davis et al. (2009) and Jacob (2008), respectively. Using interferometric observations made with the Sydney University Stellar Interferometer, they found $R = 169 \pm 8\,R_\odot$ for l Car and $R = 39 \pm 6\,R_\odot$ for η Aql, adopting a constant projection factor $p = 1.30$. We rescaled their estimations using our projection factor and obtained $R = 177 \pm 8\,R_\odot$ for l Car, which is in agreement with our result within 0.9 σ, while we are not in agreement with the radius of η Aql, $R = 41 \pm 6\,R_\odot$.

6 THE PERIOD–RADIUS RELATION

Since the radii obtained in this work are consistent with those available in the literature, we have investigated the period–radius relation for the present data set.

In order to derive the period–radius relation, we neglected the first overtone pulsators, since these objects have, at fixed period, systematically larger radii than fundamental pulsators. To pinpoint first overtone pulsators in our sample, we followed the classification given by Fernie et al. (1995). Data plotted in Fig. 8 show the radii for the entire Cepheid sample. The different colours mark Cepheids in different types of binary systems. Following the classification suggested by Szabados (2003), the black circles display single stars and visual binaries (V), the red points show the spectroscopic binaries (B), the blue points the spectroscopic binaries with known orbits (O) and the magenta points mark the binaries with photometric companions, but their binarity has to be confirmed (b), while the green circles show the position of the first overtone pulsators. We ended up with a sample of 56 Cepheids and they have been used to derive a new period–radius relation for Galactic Cepheids.

We performed a linear fit in the form $\log R = a\log P + b$, with the radius in solar units. Finally, by using $p = 1.36$, we have found the following relations:

$$\log R = (0.69 \pm 0.03)\log P + (1.17 \pm 0.03) \quad (12)$$

$$\log R = (0.73 \pm 0.03)\log P + (1.14 \pm 0.03), \quad (13)$$

in the case without and with the ΔB term, respectively. The standard deviation of the above period–radius relations is 0.06 dex. A glance at the data plotted in Fig. 8 indicates that a significant fraction of the scatter is due to binaries. The flux of the companions affects the radius estimates. This effect is more significant in optical and in ultraviolet bands than in near-infrared bands, because the Cepheid companions are typically blue stars (see e.g. Szabados 2003). In order to provide a tighter period–radius relation, we neglected all the spectroscopic binaries from the fit (types B and O of the above classification) and the first overtone candidate X Sct (see Section 6.1). The final sample reduces to 26 Cepheids and the corresponding period–radius relations for $p = 1.36$ are the following:

$$\log R = (0.71 \pm 0.03)\log P + (1.16 \pm 0.03) \quad (14)$$

$$\log R = (0.75 \pm 0.03)\log P + (1.13 \pm 0.03), \quad (15)$$

with an rms of 0.04 and 0.03 dex in the case without and with the ΔB term, respectively. The exclusion of the binary stars does not affect significantly the coefficients of the period–radius relation, but it significantly decreases the scatter of the linear fit.

The fitted equations for the case $p = 1.27$ are the following:

$$\log R = (0.71 \pm 0.03)\log P + (1.13 \pm 0.03) \quad (16)$$

$$\log R = (0.75 \pm 0.03)\log P + (1.10 \pm 0.03) \quad (17)$$

for the case without and with the ΔB term, respectively. The rms errors of these relation are the same as for the case with $p = 1.36$.

In order to validate current period–radius relations, we performed a detailed comparison with similar theoretical and empirical relations available in the literature. The zero-points and the slopes are listed in Table 4.

In order to compare theory and observations, we selected three different predictions concerning the period–radius relations at solar chemical composition. In particular, the period–radius relation provided by Alibert et al. (1999) by using linear, non-adiabatic, convective models constructed assuming a canonical (i.e. based on evolutionary models that neglect convective core overshooting during central hydrogen burning phase, rotation and mass loss) mass–luminosity relation. Moreover, we also adopted predictions provided by Bono, Caputo & Marconi (1998) and by Petroni et al. (2003) by using, non-linear, convective models constructed using both canonical and non-canonical mass-luminosity relations (mimicking the increase in luminosity caused by overshooting). To provide a robust comparison between theory and observations, we performed a new estimate of the period–radius relations using only the models of the last two data sets covering the same period range as of the current sample of Galactic Cepheids. The zero-points and the slopes listed in the first three entries of Table 4 indicate that they agree quite well with empirical period–radius relations obtained by neglecting the ΔB term. Theoretical and empirical uncertainty do not allow us to constrain the precision of the period–radius relations based on the two different projection factors.

The values given in Table 4 indicate that current period–radius relations agree, within the errors, with similar empirical estimates. On the other hand, the period–radius relation provided by Ripepi

Table 3. Radii derived in the present work compared with those previously determined by other authors (Rojo Arellano & Arellano Ferro 1994; Ruoppo et al. 2004; Barnes et al. 2005). The third column gives information on binarity according to the nomenclature from Szabados (2003): B = spectroscopic binary, b = photometric companion with no sure physical relation, O = spectroscopic binary with known orbit, V = visual binary. The Cepheids with no binarity label are bona fide single stars.

Star	Period (d)	Binarity	$\frac{R^{p=1.36}_{\rm without\Delta B}}{R_\odot}$	$\frac{R^{p=1.36}_{\Delta B}}{R_\odot}$	$\frac{R^{p=1.27}_{\rm without\Delta B}}{R_\odot}$	$\frac{R^{p=1.27}_{\Delta B}}{R_\odot}$	$\frac{R_{\rm Ruoppo04}}{R_\odot}$	$\frac{R_{\rm Barnes05}}{R_\odot}$	$\frac{R_{\rm Rojo94}}{R_\odot}$
η Aql	7.1766	B	58.2	59.0	54.3	55.1	52.6	49.2	58.1
FM Aql	6.1142	–	59.1	58.8	55.2	54.9	59.3	–	52.3
FN Aql	9.4822	b	74.1	75.5	69.2	70.5	86.5	–	–
TT Aql	13.7546	–	103.6	107.5	96.7	100.4	–	–	103.8
U Aql	7.0239	O	48.8	49.0	45.6	45.8	47.0	–	53.1
V496 Aql	6.8070	O	47.2	47.3	44.1	44.2	61.2	–	59.0
RY CMa	4.6782	B	30.1	30.4	28.1	28.4	–	–	42.2
SS CMa	12.3620	B	–	–	–	–	–	–	–
AQ Car	9.7690	–	69.3	72.3	64.7	67.5	–	–	–
ER Car	7.7187	–	56.6	58.2	52.8	54.3	–	–	–
l Car	35.5330	–	174.7	190.7	163.1	178.1	–	179.9	–
U Car	38.7681	B	–	–	–	–	–	–	–
V Car	6.6967	B	64.4	68.1	60.1	63.6	–	–	–
VY Car	18.9213	B	124.9	143.0	116.6	133.6	–	112.2	–
XX Car	15.7162	B	85.7	87.6	80.0	81.8	–	–	–
XY Car	12.4348	–	83.2	87.5	77.7	81.7	–	–	–
AZ Cen	3.2107	–	38.2	39.2	35.7	36.6	–	–	–
V Cen	5.4939	–	53.1	51.4	49.6	48.0	–	39.6	–
V339 Cen	9.4672	V	68.0	69.6	63.5	65.0	–	–	–
XX Cen	10.9558	O	61.5	63.6	57.5	59.4	–	67.2	–
AG Cru	3.8373	B	29.1	29.6	27.2	27.6	–	–	–
S Cru	4.6900	–	46.5	45.8	43.5	42.8	–	–	–
X Cru	6.2200	–	45.1	45.6	42.1	42.6	–	–	–
W Gem	7.9141	–	71.3	72.1	66.5	67.3	86.4	–	58.8
SV Mon	15.2321	–	105.5	114.5	98.5	106.9	–	–	115.4
R Mus	7.5100	B	58.1	58.2	54.2	54.4	–	–	–
UU Mus	11.6364	–	95.0	94.7	88.7	88.4	–	73.5	–
S Nor	9.7549	O	72.6	74.2	67.8	69.3	–	73.8	–
U Nor	12.6413	–	87.3	82.1	81.5	76.6	–	75.0	–
BF Oph	4.0678	B	46.8	46.6	43.7	43.5	44.8	30.1	40.3
Y Oph	17.1241	O	88.5	90.7	82.7	84.7	93.4	92.1	98.3
RS Ori	7.5668	B	55.6	56.4	51.9	52.7	–	–	–
AP Pup	5.0843	B	45.3	45.9	42.3	42.8	–	–	–
AT Pup	6.6650	B	50.0	49.3	46.7	46.0	–	–	–
RS Pup	41.3876	–	223.5	228.8	208.7	213.7	–	205.1	–
WX Pup	8.9382	–	64.5	64.7	60.2	60.4	–	–	56.8
X Pup	25.9610	–	134.5	146.7	125.6	137.0	–	–	118.5
RV Sco	6.0613	B	53.9	53.4	50.3	49.9	–	–	–
V482 Sco	4.5279	B	52.1	52.8	48.6	49.3	–	–	-
V500 Sco	9.3166	b	72.5	71.1	67.7	66.4	–	–	–
V636 Sco	6.7966	O	65.5	66.4	61.2	62.0	–	–	–
EV Sct	3.0910	B:	94.9	–	88.6	-	–	36.1	–
SS Sct	3.6712	–	39.2	38.9	36.6	36.3	44.2	–	36.0
X Sct	4.1981	b	58.4	53.5	54.5	50.0	–	–	–
Y Sct	10.3415	b	65.4	76.6	61.0	71.5	–	–	84.3
AP Sgr	5.0579	B	48.6	47.9	45.4	44.7	62.3	–	46.1
BB Sgr	6.6370	B	44.2	43.8	41.3	40.9	61.3	45.6	54.1
U Sgr	6.7449	B	64.6	65.7	60.4	61.3	82.5	49.1	55.6
W Sgr	7.5947	O	53.2	53.4	49.7	49.9	62.6	–	50.8
X Sgr	7.0122	O	54.3	52.4	50.7	48.9	59.8	–	44.1
Y Sgr	5.7733	B	55.7	55.2	52.0	51.5	56.2	–	48.3
YZ Sgr	9.5534	B	66.8	69.3	62.4	64.7	95.8	–	69.4
R TrA	3.3893	B	35.0	35.1	32.7	32.8	–	–	–
S TrA	6.3234	–	54.1	54.8	50.5	51.2	–	–	–
AH Vel	4.2271	B	55.9	51.7	52.2	48.3	-	–	-
AX Vel	2.5928	–	53.8	54.1	50.2	50.5	-	–	–
BG Vel	6.9236	b	66.0	69.7	61.6	65.1	-	–	–
RY Vel	28.1270	–	172.3	181.2	160.9	169.2	–	136.4	–

Table 3 – *continued*

Star	Period(d)	Binarity	$\frac{R^{p=1.36}_{\rm without\Delta B}}{R_\odot}$	$\frac{R^{p=1.36}_{\Delta B}}{R_\odot}$	$\frac{R^{p=1.27}_{\rm without\Delta B}}{R_\odot}$	$\frac{R^{p=1.27}_{\Delta B}}{R_\odot}$	$\frac{R_{\rm Ruoppo04}}{R_\odot}$	$\frac{R_{\rm Barnes05}}{R_\odot}$	$\frac{R_{\rm Rojo94}}{R_\odot}$
RZ Vel	20.3969	–	130.8	137.0	122.1	128.0	–	110.6	–
SX Vel	9.5499	–	64.3	65.1	60.1	60.8	–	–	–
SW Vel	23.4744	–	140.1	151.9	130.3	141.8	–	122.2	–
T Vel	4.6397	B	57.2	57.3	53.4	53.5	–	40.0	–
V Vel	4.3710	B	34.4	34.2	32.1	31.9	–	–	–

Table 4. Coefficients of the period–radius relation from the literature and of our work. The first two columns contain the slope and the intercept of the linear relation, the third column contains the reference, the fourth column the technique used to derive the period–radius relation and the last one the number of stars used in the fit.

a	*b*	Source	Method	*N*
0.71	1.14	Alibert et al. (1999)[a]	Theory (Canonical models; solar metallicity)	-
0.673 ± 0.009	1.164 ± 0.010	Bono et al. (1998)	Theory (Canonical+Non-canonical models; solar metallicity)	-
0.699 ± 0.011	1.150 ± 0.012	Petroni et al. (2003)	Theory (Canonical+Non-canonical models; solar metallicity)	-
0.75 ± 0.02	1.07 ± 0.02	Gieren et al. (1998)[b]	Surf. Brightness (variable p)	28
0.74 ± 0.03	1.12 ± 0.03	Rojo Arellano & Arellano Ferro (1994)	Surf. Brightness ($p = 1.31$)	54
0.606 ± 0.037	1.263 ± 0.033	Ripepi et al. (1997)	Surf. Brightness ($\Delta B \neq 0$, $p = 1.36$)	64
0.767 ± 0.009	1.091 ± 0.011	Kervella et al. (2004)	Interferometry ($p = 1.36$)	8
0.686 ± 0.036	1.134 ± 0.034	Groenewegen (2007)	Interferometry ($p = 1.27$)	5
0.747 ± 0.028	1.071 ± 0.025	Turner & Burke (2002)	Modified Baade–Wesselink ($p = 1.31$)	13
0.69 ± 0.09	1.18 ± 0.08	Ruoppo et al. (2004)	New CORS ($\Delta B = 0$, $p = 1.36$)	20
0.74 ± 0.11	1.19 ± 0.09	Ruoppo et al. (2004)	New CORS ($\Delta B \neq 0$, $p = 1.36$)	16
0.71 ± 0.03	1.16 ± 0.03	This Work	New CORS ($\Delta B = 0$, $p = 1.36$)	26
0.75 ± 0.03	1.13 ± 0.03	This Work	New CORS ($\Delta B \neq 0$, $p = 1.36$)	"
0.71 ± 0.03	1.13 ± 0.03	This Work	New CORS ($\Delta B = 0$, $p = 1.27$)	"
0.75 ± 0.03	1.10 ± 0.03	This Work	New CORS ($\Delta B \neq 0$, $p = 1.27$)	"

[a]Errors on the coefficients are not indicated in the original paper (Alibert et al. 1999, table 5).
[b]In order to have uniformity in the comparison with other relations, the listed uncertainties are the standard deviations on the parameters, which have been recalculated by fitting their data.

et al. (1997), using the same method, gives a smaller zero-point, but a steeper slope.

It is interesting to note that the zero-points of our relations seem to change in opposite directions by including or excluding the ΔB term with respect to those by Ruoppo et al. (2004). The main result derived from Table 4 is that the agreement of the zero-point of our relations with those of other authors (excluding the theoretical result) improves by including the ΔB term and by decreasing the projection factor from 1.36 to 1.27. Therefore, we will consider the equation

$$\log R = (0.75 \pm 0.03) \log P + (1.10 \pm 0.03) \quad (18)$$

as our best-fitting period–radius relation. A plot of our relations for $p = 1.27$ is shown in Fig. 9; the plot for $p = 1.36$ is not shown because the points are only shifted vertically by the same offset of 0.03. The projection factor does not affect the slope of the period–radius relation only when it is assumed to be constant over the period range. A visual comparison of equation 18 with other relations is shown in Fig. 10.

6.1 X Sct: a possible first overtone pulsator

To test the first overtone nature of X Sct, we estimated the radius predicted from our period–radius relations for a Cepheid with the same period: $R = 36.9^{+2.7}_{-2.4}$, for $p = 1.27$ and $R = 39.6^{+2.8}_{-2.6}$ with $p = 1.36$, in units solar radii. The values obtained from the CORS method are $R = 50.0$ and 53.5, for $p = 1.27$ and 1.36, respectively (see Table 3). They differ by more than 4σ from the predicted values, being larger, as expected for a first overtone pulsator.

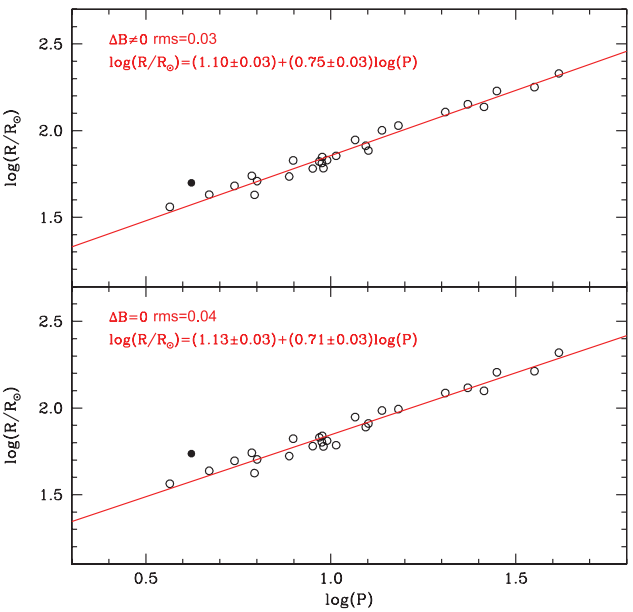

Figure 9. Period–radius relations for the final sample of Cepheids in the case with ΔB (top panel) and without ΔB (bottom panel). In each panel, the fitting equation and the scatter around the fit are also shown. The possible first overtone X Sct is also plotted (filled circle) but it is excluded from the fit.

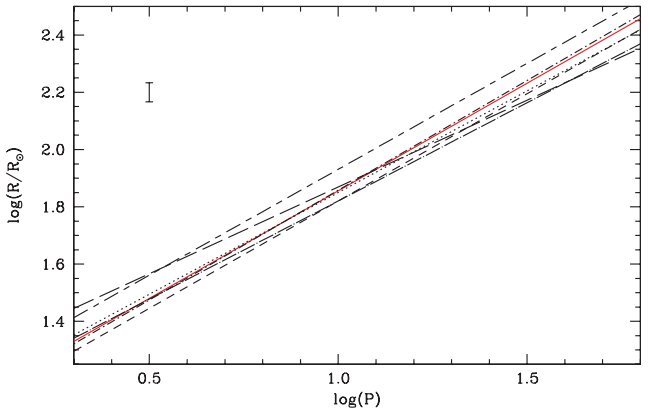

Figure 10. Our best-fitting period–radius relation (red solid line) is plotted together with those obtained by Alibert et al. (1999) (theoric relation, dot line), Gieren, Fouqué & Gomez (1998) (short dashed line), Ruoppo et al. (2004) (short dashed long dashed line), Ripepi et al. (1997) (long dashed line), Kervella et al. (2004) (dot short dashed line) and Groenewegen (2007) (dot long dashed line). The error bar represents the standard deviation of the current relation (0.03 dex).

As a further test, we have also estimated the radius predicted by the theoretical period–radius relation for first overtone Cepheids obtained by Bono et al. (2001a):

$$\log R = (0.755 \pm 0.007) \log P + (1.250 \pm 0.005) \quad (19)$$

$$\log R = (0.737 \pm 0.005) \log P + (1.219 \pm 0.004) \quad (20)$$

for canonical and non-canonical models, respectively. The radius corresponding to the period of X Sct is $R = 52.5^{+1.7}_{-1.1}$ and $R = 47.7^{+0.7}_{-0.6}$ using the canonical and the non-canonical relation, respectively. It is evident that the value obtained in the case of the canonical relation is in excellent agreement with that obtained from CORS with $p = 1.36$. The value obtained from non-canonical relation is consistent only within $\sim 3.3\sigma$ with the CORS value for $p = 1.27$.

Furthermore, we have also compared the radii of X Sct with those of the first overtone Cepheid AH Vel ($P = 4.23$) and of the fundamental pulsator V Vel ($P = 4.37$), obtained using CORS (see Table 3). As a result, we find that the radius of X Sct is much more consistent with a first overtone pulsation.

On the basis of this test, we are confident that X Sct can be a good first overtone candidate, but further analysis is required to confirm this hypothesis.

7 THE PERIOD–LUMINOSITY RELATION

The estimated radii and effective temperatures are used to derive the intrinsic luminosities of the investigated Cepheids and, in turn, their absolute visual magnitude. To this aim, we assumed the solar visual magnitude in the V band to be -26.75 (Hayes 1985), which gives an absolute visual magnitude of $+4.82$ and an absolute bolometric magnitude of $+4.75$, with a bolometric correction of -0.07. Furthermore, we calculated the bolometric correction from equation (A3). In order to evaluate the absolute magnitude uncertainty, we assumed the scatter around the fitted $\log T_{\rm eff}(V - B, U - W)$ and $\mathrm{BC}(V - B, U - W)$ surfaces as the uncertainty of the effective temperature and bolometric correction, respectively. The values of absolute magnitudes and their uncertainties, δM_V, are listed in Table 5 for the case $p = 1.27$.

The period–luminosity relation is obtained by a weighted linear fit of the relation $M_V = a\log P + b$ and the resulting coefficients are listed in Table 6 together with some results from other authors. We list the coefficients obtained using both values of the projection factor, $p = 1.27$ and 1.36.

As for the period–radius relation, the projection factor influences only the zero-point of the period–luminosity relation, leaving the slope unchanged.

From Table 6, it is evident that the slope of our period–luminosity relation is steeper than those of the relations by Fouqué et al. (2007) and Barnes et al. (2003), although they are consistent within the errors. On the other hand, it is in excellent agreement with the slope of the relations by Gieren et al. (1998) and Kervella et al. (2004).

The agreement of the zero-point with other works is better if we choose the projection factor $p = 1.27$, while in the case with $p = 1.36$ the period–luminosity relation seems to make Cepheids too luminous, particularly if we compare our relation with that found by Fouqué et al. (2007) or Gieren et al. (1998). We note that the systematic errors on the zero-point of the period–luminosity relations obtained for the two values of p is $\sim$0.15 mag, i.e. comparable with the statistical error on the zero-point itself.

A plot showing the comparison of our period–luminosity relation ($p = 1.27$) with those from Barnes et al. (2003), Kervella et al. (2004), Fouqué et al. (2007) and Gieren et al. (1998) is represented in Fig. 11.

Using the V-band absolute magnitudes and the intensity−mean ($\langle V\rangle - \langle I_C\rangle$) colour tabulated in Groenewegen (1999) for all our Cepheids, except for V500 Sco, W Gem, WX Pup, X Cru and Y Sct, for which we used the values from Caldwell & Coulson (1987), we derived the reddening free Wesenheit magnitude $W_{VI_C} = M_V - R_{VI_C}(\langle V\rangle - \langle I_C\rangle)$, where the colour coefficient $R_{VI_C} = 2.55$ is adopted from Caputo, Marconi & Musella (2000) (see Table 5 for W_{VI_C} values and their uncertainty δW_{VI_C}). The Period–Wesenheit relation, $W_{VI_C} = a \log P + b$, has been derived through a weighted linear fit using both values of the projection factor; the results are listed in Table 6 together with those obtained from Fouqué et al. (2007) and Benedict et al. (2007).

The slope of our Wesenheit relation is in agreement with the results from other authors, using both values of the projection factor. The variation of the projection factor influences the zero-point, which, for $p = 1.36$ seems to be too luminous, up to 0.46 mag if we consider the one by Fouqué et al. (2007). This result, obviously, reflects the behaviour of the obtained period–luminosity relation (see above). For $p = 1.27$, the Wesenheit zero-point results to be brighter by 0.20 mag than the one by Benedict et al. (2007) and by 0.31 mag than the one by Fouqué et al. (2007).

The implications of these results for the extragalactic distance scale calibration will be addressed in a forthcoming paper (Molinaro et al., in preparation).

8 CONCLUSIONS

In this work we have developed a modified version of the CORS method in the Walraven filters, following the approach already adopted by Ruoppo et al. (2004) in the Strömgren system, to derive the radii of a sample of 63 Galactic Cepheids observed in the Southern hemisphere. The adopted photometric data are the results of an extensive observational program (Walraven et al. 1964; Pel 1976; Pel & Lub 2007), whereas for the radial velocities we have used data available in the literature from various authors.

The observations were performed in the Walraven five-bands system (V, B, L, U, W) well suited to measure spectral characteristics of

Table 5. The data used to fit the period–luminosity and Period–Wesenheit relations are listed for the Cepheids of our sample. The absolute magnitudes M_V used to derive the Wesenheit magnitudes are calculated as described in the text, while the $(\langle V\rangle - \langle I_C\rangle)$ colour in the last column is from Groenewegen (1999). For V500 Sco, W Gem, WX Pup, X Cru and Y Sct, the $(\langle V\rangle - \langle I_C\rangle)$ colour is not available in Groenewegen (1999), and we have used the value from Caldwell & Coulson (1987).

Star name	Period (d)	$T_{\rm eff}$ (K)	M_V (mag)	δM_V (mag)	W_{VI_C} (mag)	δW_{VI_C} (mag)	$(\langle V\rangle - \langle I_C\rangle)$ (mag)
FM Aql	6.11423	5746	−3.50	0.17	−5.60	0.18	1.531
FN Aql	9.48224	5731	−4.22	0.18	−6.24	0.19	1.389
TT Aql	13.7546	5293	−4.35	0.19	−6.65	0.19	1.409
AQ Car	9.76896	5627	−4.15	0.18	−6.12	0.19	0.982
ER Car	7.7187	5642	−3.78	0.20	−5.69	0.21	0.865
l Car	35.5330	4843	−5.35	0.22	−7.93	0.22	1.177
XY Car	12.43483	5503	−4.41	0.19	−6.55	0.19	1.342
V Cen	5.49392	6069	−3.62	0.17	−5.33	0.17	1.041
V339 Cen	9.4672	5591	−4.07	0.18	−6.13	0.19	1.314
S Cru	4.68997	5956	−3.27	0.17	−4.98	0.17	0.846
X Cru	6.219970	5716	−3.50	0.19	−5.44	0.20	1.090
W Gem	7.914130	5854	−4.03	0.18	−5.90	0.18	1.043
SV Mon	15.2321	5391	−4.63	0.19	−6.80	0.20	1.119
UU Mus	11.63641	5648	−4.46	0.19	−6.47	0.19	1.294
U Nor	12.64133	5476	−4.41	0.19	−6.66	0.19	1.874
RS Pup	41.3876	5087	−5.91	0.22	−8.41	0.23	1.531
X Pup	25.9610	5368	−5.46	0.21	−7.69	0.21	1.365
WX Pup	8.938250	5809	−4.18	0.18	−6.07	0.18	1.108
V500 Sco	9.316650	5828	−4.28	0.18	−6.25	0.19	1.527
SS Sct	3.671253	5970	−2.88	0.16	−4.65	0.17	1.086
Y Sct	10.341504	5523	−4.14	0.18	−6.43	0.19	1.810
S TrA	6.32344	5810	−3.62	0.17	−5.40	0.18	0.796
RY Vel	28.1270	5411	−5.65	0.21	−7.86	0.21	1.532
RZ Vel	20.3969	5316	−5.01	0.20	−7.18	0.21	1.208
SX Vel	9.54993	5992	−4.46	0.21	−6.15	0.22	0.996
SW Vel	23.4744	5355	−5.29	0.21	−7.46	0.21	1.272

Table 6. Coefficients of the period–luminosity and of the Period–Wesenheit relations obtained in this work and from other authors.

Band	a	b	rms	Source
V	-2.77 ± 0.07	-1.29 ± 0.08	0.20	(Gieren et al. 1998)
V	-2.77 ± 0.07	-1.44 ± 0.10	–	(Kervella et al. 2004)
V	-2.68 ± 0.08	-1.27 ± 0.02	0.17	(Fouqué et al. 2007)
V	-2.69 ± 0.17	-1.47 ± 0.28	0.19	(Barnes et al. 2003)
V	-2.78 ± 0.11	-1.57 ± 0.11	0.13	This Work (p = 1.36)
V	-2.78 ± 0.11	-1.42 ± 0.11	0.13	This Work (p = 1.27)
W_{VI_C}	-3.48 ± 0.07	-2.41 ± 0.02	0.17	(Fouqué et al. 2007)
W_{VI_C}	-3.34 ± 0.17	-2.52 ± 0.17	0.09	(Benedict et al. 2007)
W_{VI_C}	-3.50 ± 0.07	-2.87 ± 0.07	0.09	This Work ($p = 1.36$)
W_{VI_C}	-3.50 ± 0.07	-2.72 ± 0.07	0.09	This Work ($p = 1.27$)

stars like Cepheids and RR Lyrae. Even though the Walraven photometric system is not available in modern observational facilities, the possibility to use, in the near future, the tunable filters opens a new path towards the performance of Cepheid observations in the Walraven bands. Since new stellar atmosphere model colours in the Walraven photometric system were available from Castelli (1999), we have been able to calibrate the surface brightness function using $(V - B)$ and $(U - W)$ colours, in order to apply the complete CORS method, including the ΔB term (equation 2).

The comparison of temperature curves for some Cepheids of our sample with the temperature values obtained from spectroscopy has revealed that the $(V - B)$ Walraven colour is a very good temperature indicator, whereas a worse agreement is found for the gravity curves, probably due to a lower accuracy in the measurement of the W-band flux.

In this work, we are able to accurately calibrate the surface brightness and to derive the radius even for Cepheids with $P \sim 40$ d. The presence of long-period stars in our sample allowed us to better constrain the coefficients of the period–radius relation. In order to derive the period–radius relation, we have considered only single stars, excluding binaries, since orbital motion and/or the influence of the flux of a companion could affect the radius derivation. Furthermore, we have also excluded first overtone pulsators. Our final sample thus reduces to 27 Cepheids.

In order to take account of the uncertainty in the projection factor value, we have considered two possible values, $p = 1.27$ and 1.36, chosen in order to include the range of values found in the literature.

The period–radius relations obtained in the present work are the following:

$$\log R = (0.75 \pm 0.03) \log P + (1.10 \pm 0.03) \tag{21}$$

$$\log R = (0.75 \pm 0.03) \log P + (1.13 \pm 0.03), \tag{22}$$

for $p = 1.27$ and 1.36, respectively. We excluded X Sct from the fit because of its large deviation ($>4\sigma$). We investigated the hypothesis that it can be an unknown first overtone Cepheid and our results suggest that it is a good candidate, but further analysis is required.

The comparison with independent results in the literature has shown that the agreement with the slope of our period–radius relations improves including the ΔB term. The only exception is the period–radius relation by Ripepi et al. (1997), who find a flatter slope using the surface brightness technique. Furthermore, the uncertainties in our relations are of the same order of magnitude or even smaller than those obtained using the infrared data. The zero-point of our relation decreases from $b = 1.13$ to 1.10 by varying the

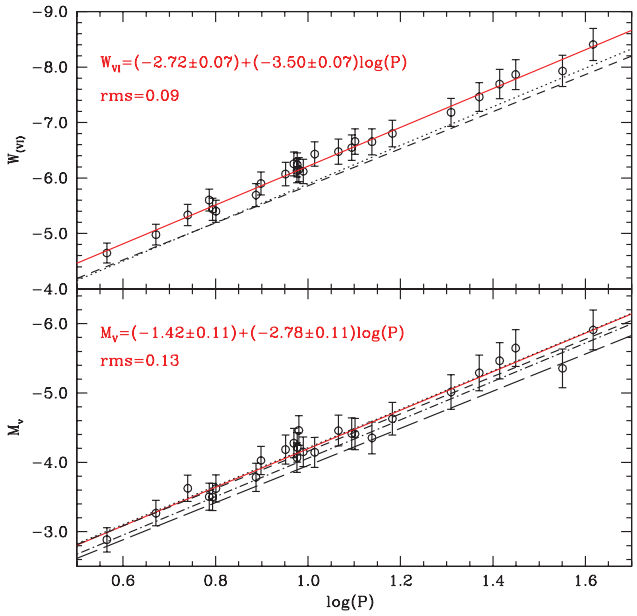

Figure 11. Bottom panel: our period–luminosity relation ($p = 1.27$) (red solid line) is plotted together with those obtained by Kervella et al. (2004) (dotted line), Barnes et al. (2003) (short dashed line), Fouqué et al. (2007) (long dashed line) and Gieren et al. (1998) (dot short dashed line). Upper panel: the Period-Wesenheit relation obtained using the projection factor $p = 1.27$ (red solid line). The other two plotted fits are from Fouqué et al. (2007) (dotted line) and Benedict et al. (2007) (short dashed line). The rms around the fitted relations are indicated in both panels.

projection factor from $p = 1.36$ to 1.27, providing a better agreement with several authors. Therefore, we consider $\log R = (0.75 \pm 0.03)\log P + (1.10 \pm 0.03)$, obtained for $p = 1.27$, as our best-fitting period–radius relation.

This result is also confirmed by the study of the period–luminosity relation. The comparison with the results of other authors (Gieren et al. 1998; Barnes et al. 2003; Kervella et al. 2004; Fouqué et al. 2007) shows that the agreement improves by decreasing the projection factor values from 1.36 to 1.27. Thus, we decided to keep the value $p = 1.27$ and considered the corresponding period–luminosity relation as the best-fitting one:

$$M_V = (-2.78 \pm 0.11)\log P - (1.42 \pm 0.11) \quad (23)$$

with a scatter of 0.13 mag, which is smaller than other works.

In order to exclude possible uncertainty in the reddening, we also derived the Period–Wesenheit relation. As expected from our findings about the period–luminosity relation, the result obtained with $p = 1.36$ seems to make Cepheids too luminous with respect to other results in the literature (Benedict et al. 2007; Fouqué et al. 2007). Thus we decided to keep the relation for $p = 1.27$ again as the best-fitting one:

$$W_{VI_C} = (-3.50 \pm 0.07)\log P - (2.72 \pm 0.07), \quad (24)$$

which has a scatter of 0.09 mag.

Whereas the implications of the obtained relations for distance scale applications and for the very important issue of the universality of the period–luminosity relations deserve further investigation and will be the subject of a forthcoming paper (Molinaro et al. in preparation), it is worth noting that the presented comparison with independent results has provided a test for the projection factor, suggesting a smaller value than the classical $p = 1.36$. In particular, $p = 1.27$ appears to be the most accurate, in agreement with the values obtained by Groenewegen (1999), Mérand et al. (2005) and Nardetto et al. (2007).

ACKNOWLEDGMENTS

It is a pleasure to thank the referee Dr P. Fouqué for his pertinent concerns and constructive suggestions that helped us to improve both the content and the readability of the paper.

This work has benefitted from the use of the McMaster data base (http://crocus.physics.mcmaster.ca/Cepheid/) maintained by D. Welch.

REFERENCES

Alibert Y., Baraffe I., Hauschildt P., Allard F., 1999, A&A, 344, 551
Barnes T. G., III, 2009, in Guzik J. A., Bradley P. A., eds, AIP Conf. Proc. Vol. 1170, Stellar Pulsation: Challenges for Theory and Observation. Am. Inst. Phys., New York, p. 3
Barnes T. G., Evans D. S., 1976, MNRAS, 174, 489
Barnes T. G., Moffet T. J., Slovak M. H., 1987, ApJS, 65, 307
Barnes T. G., Moffet T. J., Slovak M. H., 1988, ApJS, 66, 43
Barnes T. G., Jefferys W. H., Berger J. O., Mueller P. J., Orr K., Rodriguez R., 2003, ApJ, 592, 539
Barnes T. G., Storm J., Jefferys W. H., Gieren W. P., Fouqué P., 2005, ApJ, 631, 572
Benedict G. F. et al., 2007, AJ, 133, 1810
Bersier D., 2002, ApJS, 140, 465
Bersier D., Burki G., Mayor M., Duquennoy A., 1994, A&AS, 108, 25
Bono G., Caputo F., Marconi M., 1998, ApJ, 497, L43
Bono G., Marconi M., Stellingwerf R. F., 1999, ApJS, 122, 167
Bono G., Marconi M., Stellingwerf R. F., 2000, A&A, 360, 245
Bono G., Gieren W. P., Marconi M., Fouqué P., 2001a, ApJ, 552, L141
Bono G., Gieren W. P., Marconi M., Fouqué P., Caputo F., 2001b, ApJ, 563, 319
Bono G., Castellani V., Marconi M., 2002, ApJ, 565, 83
Caccin R., Onnembo A., Russo G., Sollazzo C., 1981, A&A, 97, 104
Caldwell J. A. R., Coulson I. M., 1987, AJ, 93, 5
Caputo F., Marconi M., Musella I., 2000, A&A, 354, 610
Castelli F., 1999, A&A, 346, 564
Coulson I. M., Caldwell A. R., Gieren W. P., 1985, ApJS, 57, 595
Davis J., Jacob A. P., Robertson J. G., Ireland M. J., North J. R., Tango W. J., Tuthill P. G., 2009, MNRAS, 394, 1620
Fernie J. D., Beattie B., Evans N. R., Seager S., 1995, Inf. Bull. Var. Stars, 4148, 1
Fouqué P., Arriagada P., Storm J., Barnes T. G. et al., 2007, A&A 476, 73
Freedman W. L. et al., 2001, ApJ, 553, 47
Gautschy A., 1987, Vistas Astron., 30, 197
Gieren W. P., 1977, A&AS, 28, 193
Gieren W. P., 1981, ApJS, 46, 287
Gieren W. P., 1985, ApJ, 295, 507
Gieren W. P., Fouqué P., Gomez M., 1998, ApJ, 496, 17
Gorynya N. A., Samus N. N., Sachkov M. E., Rastorguev A. S., Glushkova E. V., Antipin S. V., 1998, Astron. Lett., 24. 6, 815
Groenewegen M. A. T., 1999, A&AS, 139, 245
Groenewegen M. A. T., 2007, A&A 474, 975
Hayes D. S., 1985, in Hayes D. S., Pasinetti L. D., Philip A. G. D., eds, Proc. IAU Symp. 111, Calibration of Fundamental Stellar Quantities. Reidel, Dordrecht, p. 225
Imbert M., 1999, A&AS, 140, 791
Jacob A. P., 2008, PhD thesis, Univ. Sydney
Keller S. C., Wood P. R., 2006, ApJ, 642, 834
Kervella P., Bersier D., Mourand D., Nardetto N., Coudé du Foresto V., 2004, A&A, 423, 327
Lane B. F., Creech-Eakman M. J., Nordgren T. E., 2002, ApJ, 124, 541
Laney C. D., Caldwell J. A. R., 2007, MNRAS, 377, 147

Lloyd Evans T., 1980, South African Astron. Obser. Circ., 1, 257
Lub J., Pel J. W., 1977, A&A, 54, 137
Luck R. E., Andrievsky S. M., 2004, AJ, 128, 343
Marengo M., Sasselov D. D., Karovska M., Papaliolios C., Armstrong J. T., 2002, ApJ, 567, 1131
Mérand A. et al., 2005, A&A, 438, L9
Metzger M. R., Caldwell J. A. R., McCarthy J. K., Schechter P. L., 1993, ApJS, 76, 803
Nardetto N., Fokin A., Mourand D., Mathias Ph., Kervella P., Bersier D., 2004, A&A, 428, 131
Nardetto N., Mourard D., Mathias Ph., Fokin A., Gillet D., 2007, A&A, 471, 661
Nardetto N., Gieren W., Kervella P., Fouqué P., Storm J., Pietrzyski G., Mourard D., Queloz D., 2009, A&A, 502, 951
Nordgren T. E. et al., 2000, ApJ, 543, 972
Onnembo A., Buonaura B., Caccin B., Russo G., Sollazzo G., 1985, A&A, 152, 349
Pedicelli S., Lub J., Pel J. W., Lemasle B., Bono G., François P., 2008, Mem. Soc. Astron. Ital., 79, 539
Pedicelli S. et al., 2009, A&A, 504, 81
Pel J. W., 1976, A&A, 24, 413
Pel J. W., 1978, A&A, 62, 75
Pel J. W., Lub J., 2007, in Sterken C., ed., ASP Conf. Ser. Vol. 364, The Future of Photometric, Spectrophotometric, and Polarimetric Standardization. Astron. Soc. Pac., San Francisco, p. 63
Petroni S., Bono G., Marconi M., Stellingwerf R. F., 2003, ApJ, 599, 522
Ripepi V., Barone F., Milano F., Russo G., 1997, A&A, 318, 797
Ripepi V., Russo G., Bono G., Marconi M., 2000, A&A, 354, 77
Rojo Arellano E., Arellano Ferro A., 1994, Rev. Mex. Astron. Astrofís., 29, 148
Ruoppo A., Ripepi V., Marconi M., Bono G., 2004, A&A, 422, 253
Sasselov D. D., Karovska M., 1994, ApJ, 432, 367
Sollazzo C., Russo G., Onnembo A., Caccin B., 1981, A&A, 99, 66
Stibbs D. W. N., 1955, MNRAS, 115, 363
Storm J., Carney B. W., Gieren W. P., Fouqué P., Freedman W. L., Madore B. F., Habgood M. J., 2004, yCat, 341, 50521
Storm J., Gieren W. P., Fouqué P., Barnes T. G., III, Gómez M., 2005, A&A, 440, 487
Szabados L., 2003, Inf. Bull. Var. Stars, 5394
Taylor M. M., Albrow M. D., Booth A. J., Cottrell P. L., 1997, MNRAS, 292, 662
Turner D. G., Burke J. F., 2002, AJ, 124, 2931
Walraven J. H., Tinbergen J., Walraven Th., 1964, Bull. Astron. Inst. Netherlands, 17, 520
Wesselink A. J., 1946, Bull. Astron. Inst. Netherlands, 368, 91
Wilson T. D., Carter M. W., Barnes T. G., Van Citters G. W., Moffett T. J., 1989, ApJS, 69, 951

APPENDIX A: THE FIT OF THEORETICAL GRIDS

Here we show the result of the polynomial fit performed in order to express the effective temperature, $\log T_{\rm eff}$ and the effective gravity, $\log g_{\rm eff}$ as function of the $(V-B)$ and $(U-W)$ colours and the bolometric corrections, BCs, as function of temperature and gravity:

$$\log T_{\rm eff} = a_0 + a_1(V-B) + a_2(U-W) + a_3(V-B)(U-W) \quad \text{(A1)}$$

$$\log g_{\rm eff} = b_0 + b_1(V-B) + b_2(U-W)^2 + b_3(V-B)(U-W) + b_4(V-B)^2(U-W) + b_5(V-B)(U-W)^2 + +b_6(V-B)^2(U-W)^2 \quad \text{(A2)}$$

$$\mathrm{BC} = c_0 + c_1(\log T_{\rm eff}) + c_2(\log T_{\rm eff})^2 + c_3(\log g_{\rm eff}) + c_4(\log T_{\rm eff})(\log g_{\rm eff}) \quad \text{(A3)}$$

The coefficients a_i, b_i, c_i of the previous equations are listed in Table A1. The rms of the previous relations are 0.0033, 0.15 and 0.0032, respectively.

APPENDIX B: THE ANALYSIS WITH $(V-B)$–$(L-U)$ COLOURS

Fig. B1 shows the grid of models in the plane $(V-B)$–$(L-U)$ for the parameter range $5000 \leq T_{\rm eff} < 7500$ and $0.0 \leq \log g_{\rm eff} \leq 4.00$. According to the procedure described in Appendix A, we performed

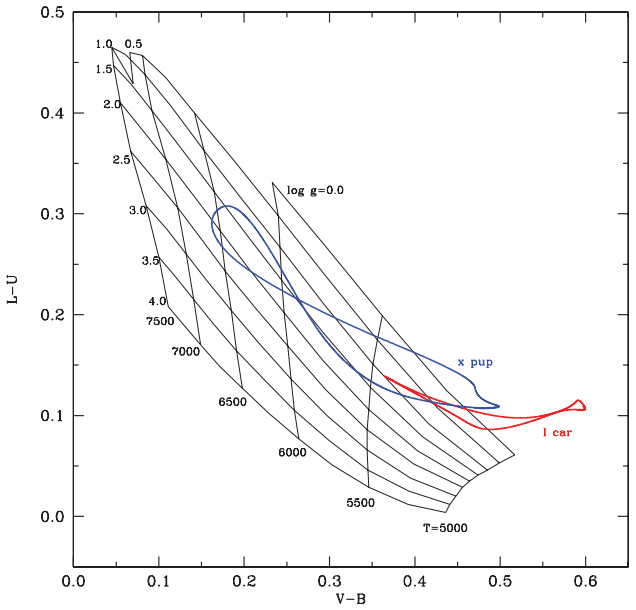

Figure B1. Grids of models in the $(V-B)$–$(L-U)$ plane for the parameter range $5000 \leq T_{\rm eff} < 7500$ and $0.0 \leq \log g_{\rm eff} \leq 4.00$. The coloured lines represent the loop of the two long period Cepheids l Car ($P = 35$ d) and x Pup ($P = 26$ d).

Table A1. Coefficients of the polynomial relations described in the Appendix A.

a_0	a_1	a_2	a_3	a_4	a_5	a_6
3.959 ± 0.004	-0.666 ± 0.012	-0.251 ± 0.013	0.82 ± 0.03			
b_0	b_1	b_2	b_3	b_4	b_5	b_6
3.21 ± 0.19	23.0 ± 3.0	-24.0 ± 2.0	-130.0 ± 18.0	59.0 ± 12	204.0 ± 27	-151.0 ± 29
c_0	c_1	c_2	c_3	c_4	c_5	c_6
85.7 ± 1.4	-44.41 ± 0.73	5.75 ± 0.10	-0.12 ± 0.02	0.035 ± 0.006		

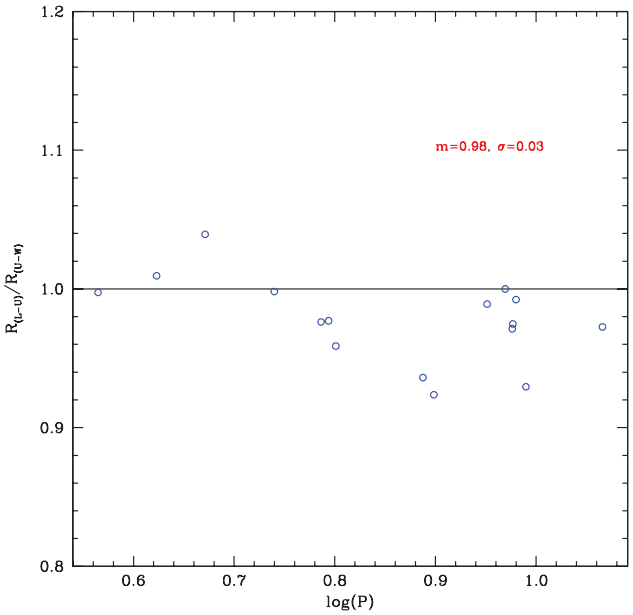

Figure B2. The ratios between the new radii obtained with $(L - U)$ colour and the old values for a sample of singular Cepheids with colour–colour loop fully contained on the $(V - B)$–$(L - U)$ grid of models. The mean ratio and the standard deviation, indicated in red, are respectively $m = 0.98$ and $\sigma = 0.03$.

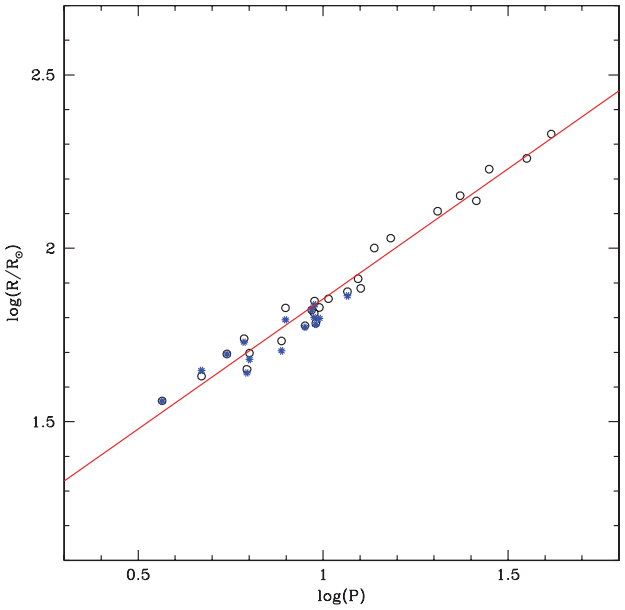

Figure B3. The period–radius relation (equation 15) is plotted together with the values of radius (blue stars) obtained with $(L - U)$ colour, for the sample of Cepheids having loop fully contained on the grid of $(V - B)$–$(L - U)$ models.

a fit of the grid using polynomial equations in the variable $(V - B)$ and $(L - U)$. For brevity, we do not give the explicit expressions of the fit, but we recall that the rms of residuals around the fit are 0.0023 and 0.14 for $\log T_{\rm eff}$ and $\log g_{\rm eff}$, respectively.

In the same graphic, the loops of the Cepheids l Car ($P = 35$ d) and X Pup ($P = 26$ d) are also plotted. Since part of the loops falls outside of the grid, we are not able to accurately estimate the structural parameters of the two stars for all phases of the pulsational cycle. The same behaviour is observed for most Cepheids with period longer than 11 d. It would be interesting to investigate about this finding in a subsequent work. A possible reason may be that the L band covers an extremely line-rich region of the spectrum. Apart from a very large number of metallic lines, it includes the higher Balmer lines and molecular lines of CN and CH. For this reason, L may be more sensitive to dynamic effects (emission components due to shock waves, enhanced and time-variable microturbulence) not included in the physics at the base of models, hence more sensitive to breakdown of the quasi-hydrostatic equilibrium assumption. The presence of molecular lines in L may also mean that the Kurucz/Castelli model atmospheres have shortcomings at the cool end of the grids that become particularly pronounced in L.

Using only the Cepheids with loops fully contained on the grids, we have estimated their radii comparing them with old values obtained using the $(U - W)$ colour. The ratios of their values, plotted in Fig. B2, show that the differences are smaller than 10 per cent, with mean ratio equal to 0.98 and a standard deviation of 0.03. We have also overplotted the new radii on the period–radius relation (equation 15) and they seem to lie on the fitted relation as shown in Fig. B3.

On the basis of these analysis, we have decided to use the $(U - W)$ colour instead of $(L - U)$.

This paper has been typeset from a TEX/LATEX file prepared by the author.